Available online at www.easdprocedia.org
EASD Procedia EURODYN (2020) 1422-1432

EASD Procedia

EURODYN 2020
XI International Conference on Structural Dynamics
M. Papadrakakis, M. Fragiadakis, C. Papadimitriou (eds.)
Athens, Greece, 23–26 November 2020

CONTROL LAW AND ACTUATOR CAPACITY EFFECT ON THE DYNAMIC PERFORMANCE OF A HYBRID MASS DAMPER; THE CASE OF ROTTWEIL TOWER

Lefteris Koutsoloukas[1], Nikolaos Nikitas[2], Petros Aristidou[3] and Christian Meinhardt[4]

[1] School of Civil Engineering, University of Leeds
LS2 9JT, Leeds, UK
cn15lk@leeds.ac.uk

[2] School of Civil Engineering, University of Leeds
LS2 9JT, Leeds, UK
N.Nikitas@leeds.ac.uk

[3] Department of Electrical Engineering & Computer Engineering and Informatics,
Cyprus University of Technology
3036 Limassol, Limassol, CY
petros.aristidou@cut.ac.cy

[4] GERB Vibration Control Systems,
Roedernallee 174-176,13407 Berlin, DE
christian.meinhardt@gerb.de

Keywords: Tall Buildings, Active/Hybrid Mass Damper, Model Predictive Control, Structural Dynamics, Vibration Mitigation

Abstract. *This paper considers different vibration control options for a real high-rise tower subjected to real wind loading. To mitigate excessive responses, the tower utilizes a hybrid passive - active control system with a relatively small actuator capacity. Firstly, the methodology for establishing a reduced order numerical model of the tower from a finite element realization is presented. Subsequently, to deal with physical constraints, a Model Predictive Control (MPC) algorithm is employed and compared to a more conventional Linear Quadratic Regulator (LQR). In both cases, the algorithms managed to keep the dynamic displacements within the set desired limit. It was concluded that, the MPC had a better performance when compared to the LQR in terms of peak amplitudes at the expense though of energy.*

ISSN:2311-9020
Peer-review under responsibility of the Organizing Committee of EURODYN 2020.
doi: 10.47964/1120.9115.19241

1 INTRODUCTION

The technological advancement and increase of cost-efficient computational power , create the ideal conditions for the broader implementation of active control systems. Traditionally, disciplines such as aerospace and automotive, have been utilizing active control schemes in order to enhance performance for a range of applications[1, 2]. Yet, active control is now also growing in disciplines that, it was not popular, or even viable, in the near past. More specifically, the recent trend of building tall and slender structures led to the development of structural control systems that utilize active components for vibration mitigation under extreme loads.

Generally speaking, active and semi-active structural control systems can achieve enhanced control performance when compared to passive equivalents. However, the performance of active control systems may be limited due to various practical and operating constraints. For the case of a mass damper such can be the actuator dynamics, mass stroke, and energy consumption. To this goal, extensive efforts have been made by the structural control research community and smart methods have been developed to minimize, if not eliminate, any performance compromising effects of constraints.

This paper will investigate the application of an active hybrid mass damper system on a real 245m tower subjected to wind loading, without accounting for any aeroelastic effects. For the control of the hybrid system, Model Predictive Control (MPC) algorithm will be used and compared to a more conventional Linear Quadratic Regulator (LQR). Previously, the MPC algorithm was investigated by Mei et al. [3, 4] for the control of the famous 76-storey benchmark building. Moreover, applications of the MPC on different control systems were practiced by Mei et al. [5, 6] for the case of a single and a three-storey structure, by Chen et al. [7] for a ten-storey structure, explaining additionally a more practical implementation of the algorithm, by Peng et al. [8] for two adjacent 20-storey buildings and by Lopez et al. [9] for a six-storey experimental structure.

Herein, the constraint effect of the actuator maximum capacity on the overall performance of the hybrid control system will be examined, and methodologies for minimizing it will be reviewed. More specifically, the actuator that was utilized on the hybrid control system of the 245m tower has a maximum force rating of 35kN, which is relatively low compared to the 180,000t tower mass. For reference and comparison, the actuators deployed for the control of the Nanjing TV tower had a capacity of 100kN [10], for the Shanghai World Financial Center Tower 142.5kN [11], for a 36-storey building reported in [12] 25.4kN, and for a benchmark cable-stayed bridge (Cape Girardeau Bridge, Missouri, USA) up to 7000kN [13] with typical values around reaching 1000kN [14]. For the 76-storey benchmark building, which is of significance to this study, the actuator capacity was limited to lower than 300kN [15], while Mei et al. [3] using the MPC algorithm, found that the maximum actuator force needed was 118kN.

2 APPLICATION DEFINITION

The 245m tower is the Rottweil Tower in Germany and was commissioned with specific requirements for experiencing limited wind-induced vibrations within certain bounds. According to wind tunnel tests, it was expected that wind speeds of the order of 15.3 – 16.7 m/s, referring to ground values at a height of 10m, could excite top floor dynamic response with amplitude of up to 750mm when no added control measure is provisioned. Such vibrations are primarily of vortex shedding type. Associated sway disturbance is anticipated to cause discomfort to the occupants and also impact the structural integrity of the tower particularly in terms of long term fatigue [16].

For ensuring comfort and safety, a limit displacement of up to 200mm was implemented and a hybrid structural control system was designed. The proposed hybrid system combines a

passive Tuned Mass Damper (TMD) with one actuator for each of the two principal directions. In reality, the passive TMD has adjustable stiffness that renders it semi-active; for simplification purposes this adaptiveness will not be considered any further in this study. Based on closed form formulas [17], a mass of 240t was opted for the TMD element of the system; this corresponds to a mass ratio of μ =1.3%. On the sensing side, the system consists of four uniaxial MEMS accelerometers which are able to capture horizontal accelerations at the top of the structure and the TMD mass. The displacements of the actuators are monitored by string pot transducers and an inductive length measuring system integrated within the linear motors [18].

3 PAPER CONTRIBUTIONS

1) Application of the MPC algorithm for the active hybrid control of a real structure and assessment of its performance by comparing it to an LQR controller
2) Optimization of the hybrid control system performance when acting in a passive-active mode of operation, taking into account its limited actuation capacity
3) Presentation of a real case-study that can become a benchmark for subsequent vibration control studies

4 SIMPLIFIED NUMERICAL MODEL DERIVATION

A detailed 3D Finite Element (FE) model of the tower, seen in Figure 1 (b), which falls very close in terms of observed and modelled frequencies, was used as the base for acquiring the reduced 2D lumped mass model shown in Figure 1 (c). In the reduction process, the entire mass of the tower, including the structural and non-structural components, was distributed evenly at the floors of the structure. This method results a diagonal mass matrix **M** of size *n x n* where, *n=34* is the considered number of lumped masses in the reduced model.

To derive the *n x n* stiffness matrix **K**, the methodology described by Qu et al., (2001) [19] was followed. Based on their methodology, the flexibility coefficients δ_{ij} of each floor were determined by evaluating the static responses of the i^{th} floor of the original FE model to unit horizontal forces at each node of the j^{th} floor, with $i,j= 1, 2, 3, \ldots ,n$. Thus, the flexibility matrix was constructed, and the stiffness matrix **K** was obtained by inverting it.

The damping matrix $\hat{\mathbf{C}}$ of size *n x n* for the lumped mass model was determined using the Rayleigh approximation whereby $\hat{\mathbf{C}}$ is described by Eq. 1. Parameters α and β are the mass and stiffness proportional damping coefficients, respectively and were obtained based on critical damping ratio of 1% for modes 1 and 5. For this assumption, α and β are becoming $2.11\text{x}10^{-2}$ and $5.26\text{x}10^{-4}$, respectively.

$$\hat{\mathbf{C}} = \alpha\mathbf{M} + \beta\mathbf{K} \qquad (1)$$

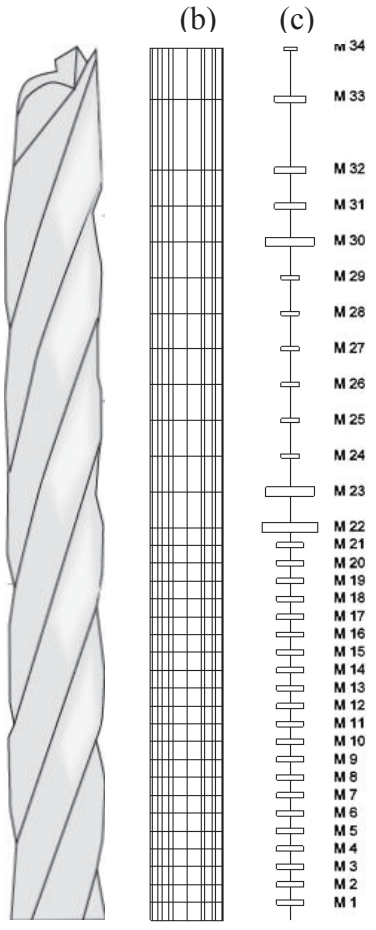

Figure 1: Three models of the tower: (a) architectural model, (b) original 3D FE model, (c) lumped mass model with equivalent masses

5 EQUATIONS OF MOTION FOR THE SYSTEM

The matrix equation of motion for the system in-hand can be expressed by Eq. 2. The nominal properties of the TMD were added to the mass **M**, stiffness **K,** and damping $\hat{\mathbf{C}}$**,** matrices derived in section 4, resulting to matrix sizes n_{tmd} *x* n_{tmd} where, n_{tmd} = 35. **f**(*k*) is an *r*-size vector which contains the external excitations applied on the structure, **u**(*k*) is the active *m*-size control force vector and **s**(*k*) is the n_{tmd} -size displacement vector, all at discrete time *k*. $\hat{\mathbf{D}}$ is the n_{tmd} *x m* matrix that describes how the control force is acting on the system, and **H** is the n_{tmd} *x r* matrix that describes how the excitation inputs are exciting the system.

$$\mathbf{M}\ddot{\mathbf{s}}(k)+\hat{\mathbf{C}}\dot{\mathbf{s}}(k)+\mathbf{K}\mathbf{s}(k)=\hat{\mathbf{D}}\mathbf{u}(k)+\mathbf{H}\mathbf{f}(k) \tag{2}$$

The equivalent spate-space equations are formulated as follows,

$$\dot{\mathbf{x}}(k)=\mathbf{A}\mathbf{x}(k)+\mathbf{B}\mathbf{u}(k)+\mathbf{G}\mathbf{f}(k),\qquad \mathbf{x}(0)=\mathbf{x}_0, \tag{3}$$

$$\mathbf{y}(k)=\mathbf{C}\mathbf{x}(k)+\mathbf{D}\mathbf{u}(k) \tag{4}$$

where **y**(*k*) represents the measured outputs, **C** is the output matrix, **D** is the feedthrough matrix, $\mathbf{x}_0$ is the initial point and,

$$\mathbf{x}(k)=\begin{bmatrix}\mathbf{s}(k)\\ \dot{\mathbf{s}}(k)\end{bmatrix},\ \mathbf{A}=\begin{bmatrix}\mathbf{0} & \mathbf{I}\\ -\mathbf{M}^{-1}\mathbf{K} & -\mathbf{M}^{-1}\hat{\mathbf{C}}\end{bmatrix},\ \mathbf{B}=\begin{bmatrix}\mathbf{0}\\ \mathbf{M}^{-1}\hat{\mathbf{D}}\end{bmatrix},\ \mathbf{G}=\begin{bmatrix}\mathbf{0}\\ \mathbf{M}^{-1}\mathbf{H}\end{bmatrix} \tag{5}$$

6 MPC STATE SPACE FORMULATION

This section includes the general formulation of MPC in state-space form. It is noted that derivation of the LQR controller, used only for comparisons, can be found in [20] and is not shown here for brevity. The MPC is based on an iterative, finite-horizon optimization of a plant. It receives a reference trajectory as the target output of the process. The overview of the algorithm is seen in Figure 2 [21]. The MPC computes a sequence of control actions **u** over a control horizon *q*, that will achieve the optimal behavior of the dependent variables **x** of the system, over a prediction horizon *p* (*p*≥*q*). It then implements only the first computed action **u**(*k*), measures the response of the system **y**(*k*), and repeats the previous process.

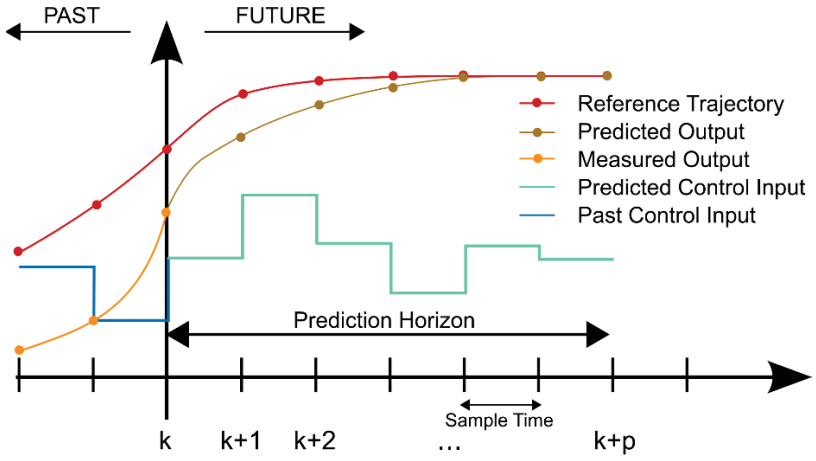

Figure 2: Basic concept for Model Predictive Control with q=p [22]

Since there might be inaccuracies and statistical noise in the measurements received and model used, a Kalman estimator is employed both for estimating the current state $\mathbf{x}(k)$ but also for the predictions needed for the MPC [21]. Eq. 6 describes how the estimates of the current state, $\hat{\mathbf{x}}(k|k-1)$, is generated by the Kalman estimator.

$$\hat{\mathbf{x}}(k \mid k-1) = \mathbf{\Phi}\hat{\mathbf{x}}(k-1 \mid k-2) + \mathbf{\Gamma}\mathbf{u}(k-1) + \mathbf{L}\mathbf{e}(k-1) \tag{6}$$

where, $\mathbf{L}$ the estimator gain matrix, and $\mathbf{C}$ the output matrix. $\mathbf{\Phi}$, $\mathbf{\Gamma}$, and $\mathbf{e}(k)$ are defined in Eq.7 for the control interval T.

$$\mathbf{\Phi} = e^{\mathbf{A}T}, \qquad \mathbf{\Gamma} = e^{\mathbf{A}T}\int_0^T e^{-\mathbf{A}x}dx, \qquad \mathbf{e}(k) = \mathbf{y}(k) - \mathbf{C}\hat{\mathbf{x}}(k \mid k-1) - \mathbf{D}\mathbf{u}(k \mid k) \tag{7}$$

The future state predictions $\hat{\mathbf{z}}(k|k+j)$ for $j=1,2,\ldots p$, are similarly determined by:

$$\hat{\mathbf{z}}(k \mid k+j) = \mathbf{\Phi}\hat{\mathbf{z}}(k+j-1) + \mathbf{\Gamma}\mathbf{u}(k+j-1 \mid k) + \mathbf{L}\mathbf{e}_f(k) \tag{8}$$

where,

$$\hat{\mathbf{z}}(k) = \hat{\mathbf{x}}(k \mid k-1) \tag{9}$$

Unlike the LQR, the constrained MPC is able to take into account bounds on the control actions $\mathbf{u}$ and future states $\hat{\mathbf{z}}$. With the target states and inputs defined by $\mathbf{z}_s$ and $\mathbf{u}_s$, respectively, the MPC objective for time instance k becomes:

$$\underset{\mathbf{u}}{Min}\, J(k) \tag{10}$$

where,

$$J(k) = [\hat{\mathbf{z}}(k+p) - \mathbf{z}_s(k)]^{\mathrm{T}}\mathbf{w}_\infty[\hat{\mathbf{z}}(k+p) - \mathbf{z}_s(k)] + \sum_{j=1}^{p}[\hat{\mathbf{z}}(k+j) - \mathbf{z}_s(k)]^{\mathrm{T}}\mathbf{w}_x[\hat{\mathbf{z}}(k+j) - \mathbf{z}_s(k)] +$$
$$\sum_{j=0}^{q-1}[\mathbf{u}(k+j \mid k) - \mathbf{u}_s(k)]^{\mathrm{T}}\mathbf{w}_u[\mathbf{u}(k+j \mid k) - \mathbf{u}_s(k)] \tag{11}$$

In Eq. 11, $\mathbf{w}_x$ and $\mathbf{w}_u$ are positive definite matrices representing the state error and the input weighting, respectively. $\mathbf{w}_\infty$ represents the terminal state matrix and can be found by solving the discrete Lyapunov equation [21]. The minimization problem is subject to constraints from Eqs. 6-9 (state estimation and predictions), alongside with the control input constraints shown in Eqs. 12-14.

$$\mathbf{u}(k+q \mid k) = \mathbf{u}(k+q+1 \mid k) = \ldots = \mathbf{u}(k+p-1 \mid k) = \mathbf{u}(k+q-1 \mid k) \tag{12}$$

$$\mathbf{u}_{\min} \le \mathbf{u}(k+j \mid k) \le \mathbf{u}_{\max} \qquad j=0, 1, 2 \ldots, q-1. \tag{13}$$

$$\Delta\mathbf{u}_{\min} \le \Delta\mathbf{u}(k+j \mid k) \le \Delta\mathbf{u}_{\max} \qquad j=0, 1, 2 \ldots, q-1. \tag{14}$$

7 PRELIMINARY RESULTS

An MPC and an LQR controller have been designed for the dynamic (response) control of the Rottweil tower, when subjected to real wind loading, using a hybrid mass damper. The passive-active mode of operation implies that, the hybrid mass damper is acting passively, and the actuators are constantly adding forces on top. A Kalman filter was used in both control cases for the state estimation using the four actual sensors located on the structure. Both controllers were designed in Matlab®. The MPC controller was realised based on the YALMIP toolbox, which is mainly used for treating prototype optimization problems [23]. The toolbox can utilize several solvers to carry out the optimization. In this study, the Gurobi optimizer was used [24]. Moreover, a hard constraint was introduced in the optimization procedure for the control input ($\mathbf{u}_k$) where, $\mathbf{u}_{min}$ and $\mathbf{u}_{max}$ were set to -35kN and 35kN respectively, T was set to 100ms and $\mathbf{z}_s$, $\mathbf{u}_s$ and $\mathbf{w}_\infty$ were set to 0. It is noted that the limit for the actuator capacity in the case of the LQR was introduced artificially in the simulation.

To simulate the dynamics of wind loading, a stochastic gust loading based on the Davenport spectrum with a linearly superimposed resonant, vortex shedding-type contribution were used [16]. The wind excitation caused a peak displacement of 248.2mm at the top floor in the case of no TMD installation.

Table 1 summarizes the maximum displacements of the floors of the structure in the uncontrolled and controlled cases. As it can be seen, both algorithms managed to reduce the structural responses at the top of the tower within the desired limit (200mm). However, the MPC had better performance than the LQR in controlling floor displacements throughout.

Floor No.	No control s(mm)	TMD s(mm)	LQR s(mm)	MPC s(mm)
1	1.8	1.6	1.4	1.35
10	53.2	48.3	42.4	40.6
20	160.7	146.1	128.1	122.6
34	248.2	225.7	197.9	189.4

Table 1: Maximum responses for the uncontrolled, TMD, LQR and MPC schemes

Based on the analysis, the maximum force exerted by the TMD without and with the active control component was 135.5kN and 170.5kN, respectively. Figures 3, 4 and 5 show displacement time series of the top floor of the structure with and without control, for the different control variants.

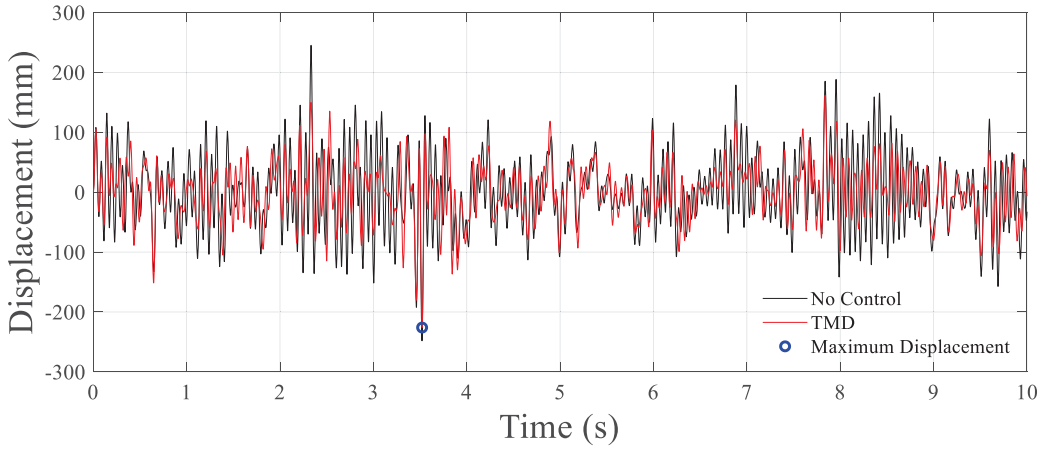

Figure 3: Displacement – Time graph for the uncontrolled case and the structure with a TMD

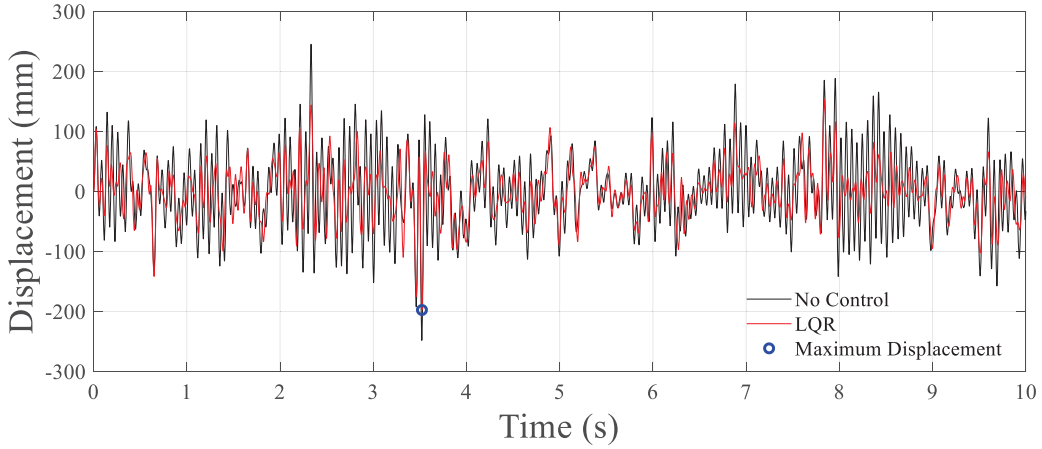

Figure 4: Displacement – Time graph for the uncontrolled case and the structure with active (LQR) control

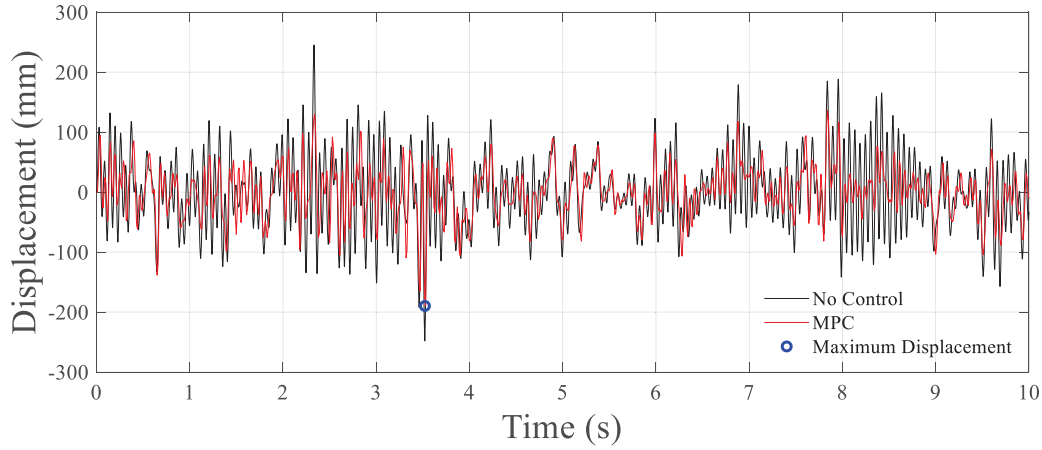

Figure 5: Displacement – Time graph for the uncontrolled case and the structure with active (MPC) control

It is observed that the active control algorithms can limit displacements even when, the actuator capacity is constrained to a fraction of the TMD passive force, as seen in Figures 6. To further asses the relative performance of the two controllers, while on a mixed passive-active

mode of operation, the actuator power, or else the product of actuator force and velocity was considered. It was found that the maximum power needed when using the LQR controller was lower than the equivalent needed for the MPC controller, as seen in Figure 7. When considering the average power the same relation pertains is with differences also in terms of extreme values and positive to negative value balance.

As such, when the hybrid system is acting in the considered passive-active mode, the MPC algorithm had the best performance on limiting dynamic displacements but in the expense of having higher energy demands than the LQR. This makes the consideration of also other modes of operation, (e.g. revised passive-active mode, having the active forces acting only when the passive forces are not sufficient and semi-active – active mode where performance can be gained at lower energy consumption) vital prior to holistically optimising the hybrid mass damper's performance, through control law considerations alone.

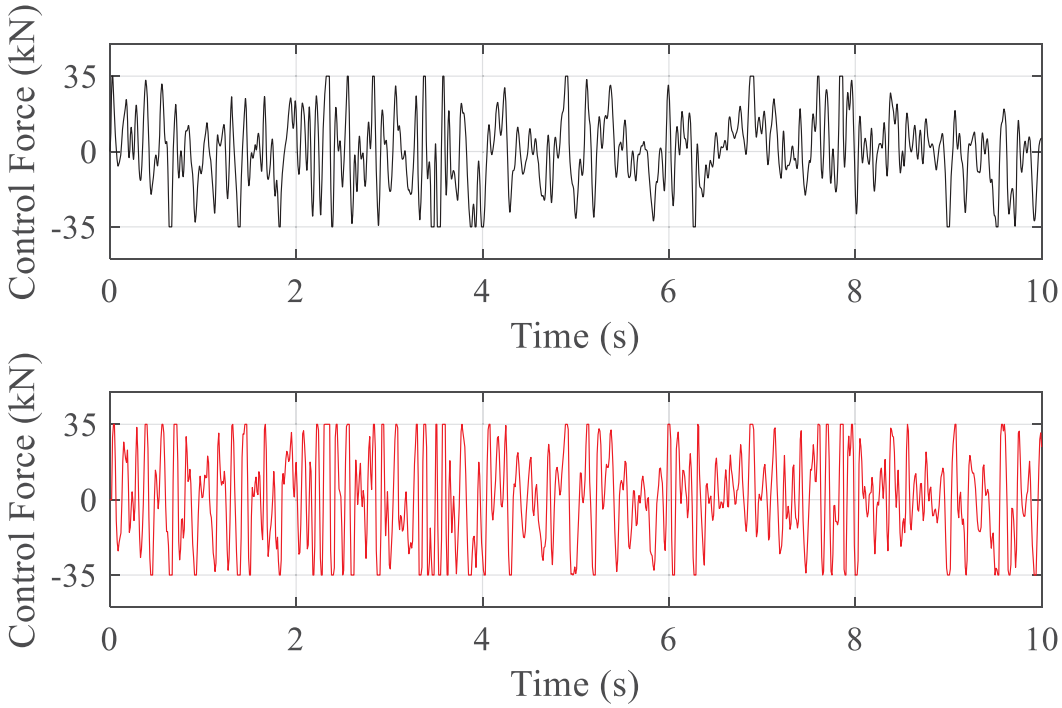

Figure 6: Active control forces when using the LQR (top) and the MPC (bottom) algorithms

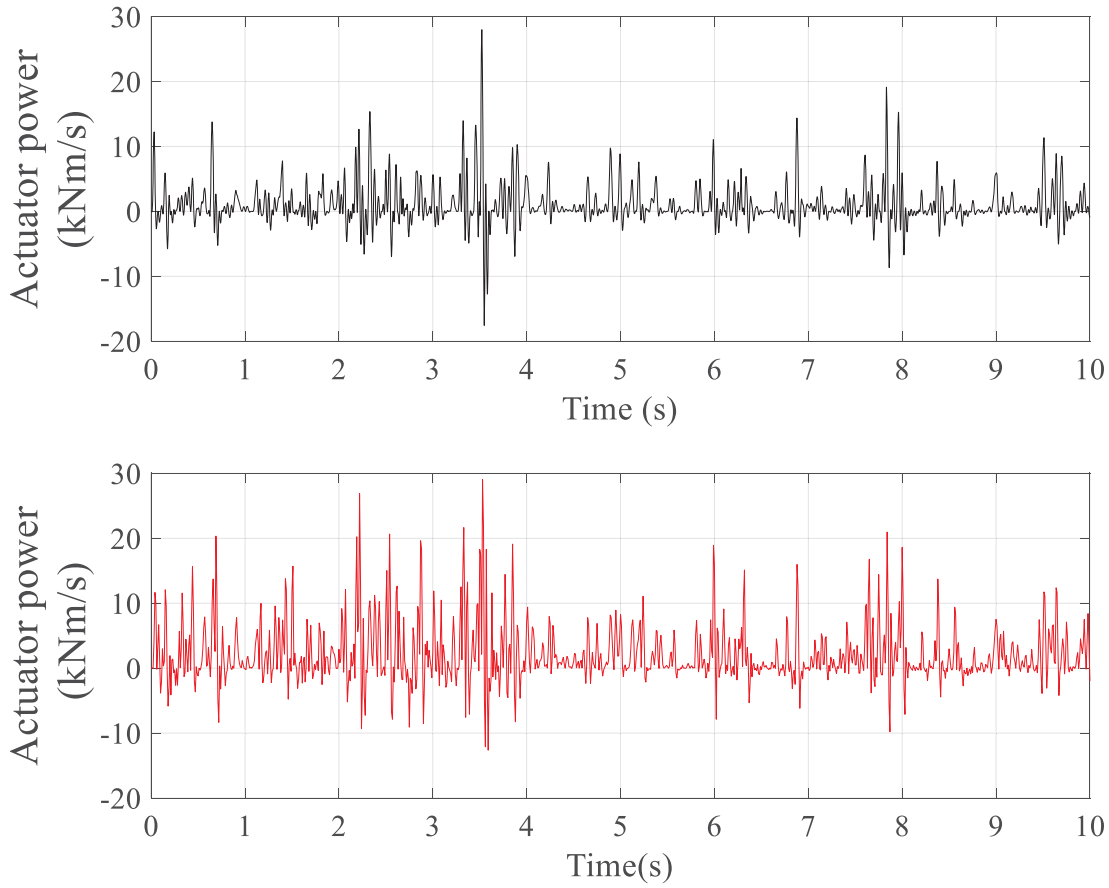

Figure 7: Actuator power when using the LQR (top) and the MPC (bottom) algorithms

8 CONCLUSIONS AND FUTURE RECOMMENDATIONS

This paper presented a real case-study which can introduce a new benchmark problem for structural control purposes. After deriving a reduced order model based on a detailed finite element model of the Rottweil tower, two control laws, namely the LQR and MPC, were applied and their performance was compared, for a passive-active mode of operation of a hybrid mass damper installation.

Based on the analysis it was found that the uncontrolled case-study building, under strong wind excitation developed dynamic displacements with maximum amplitude of 248.2mm at the top floor. When adding a perfectly tuned passive TMD the same displacement reduced to 225.7mm. In both cases, the displacements exceeded a notional serviceability limit that was set at 200mm. When considering active contribution in the control, the LQR algorithm reduced response to 197.9mm whereas, the MPC achieved 189.4mm. It was concluded that, in both cases, the algorithms managed to keep the dynamic displacements within the desired limit however, the MPC had a better dynamic reduction performance than the LQR. Still, the average energy needed for the two controllers was lower for the LQR, leading to the need for holistically optimising performance on mixed objectives.

Future work would involve semi-active – active mass damper devices, consideration of actuator dynamics and different modes-of-operation for the hybrid setup towards achieving a low energy-consumption scheme. Lastly, state-of-the-art data driven controllers, based on Artificial

Intelligence, should also enter the comparison against the presented conventional controllers in order to evaluate any performance gains.

9 ACKNOWLEDGEMENT

The authors would like to thank GERB for providing the hybrid system specifications, the FE models of the tower and the wind loading profiles. Additionally, the authors would like to thank the University of Leeds for providing the scholarship to the 1st author for conducting his PhD studies.

10 REFERENCES

[1] D. Zhao, Z. Lu, H. Zhao, X. Y. Li, B. Wang, and P. Liu, A review of active control approaches in stabilizing combustion systems in aerospace industry, *Progress in Aerospace Sciences*, 97, April 2017, 2018.

[2] P. N. Samarasinghe, W. Zhang, and T. D. Abhayapala, Recent Advances in Active Noise Control Inside Automobile Cabins: Toward quieter cars, *IEEE Signal Processing Magazine*, 33, 6, 2016.

[3] G. Mei, A. Kareem, and J. C. Kantor, Model Predictive Control of Wind-Excited Building: Benchmark Study, *Journal of engineering mechanics*, 2004.

[4] G. Mei, A. Kareem, and J. C. Kantor, Model Predictive Control For Wind Excited Buildings : A Benchmark Problem, *14th Engineering Mechanics Conference*, 2000.

[5] G. Mei, A. Kareem, and J. C. Kantor, Real-time model predictive control of structures under earthquakes, *Earthquake Engineering and Structural Dynamics*, 30, 7, 2001.

[6] G. Mei, A. Kareem, and J. C. Kantor, Model predictive control of structures under earthquakes using acceleration feedback, *Journal of Engineering Mechanics*, 128, 5, 2002.

[7] Y. Chen, S. Zhang, H. Peng, B. Chen, and H. Zhang, A novel fast model predictive control for large-scale structures, *JVC/Journal of Vibration and Control*, 23, 13, 2017.

[8] H. Peng, Y. Chen, E. Li, S. Zhang, and B. Chen, Explicit expression-based practical model predictive control implementation for large-scale structures with multi-input delays, *JVC/Journal of Vibration and Control*, 24, 12, 2018.

[9] F. Lopez-Almansa, R. Andrade, J. Rodellar, and A. M. Reinhorn, Modal predictive control of structures. II: Implementation, *Journal of Engineering Mechanics*, 120, 8, 1994.

[10] H. Cao, A. M. Reinhorn, and T. T. Soong, Design of an active mass damper for a tall TV tower in Nanjing, China, *Engineering Structures*, 20, 3, 1998.

[11] X. Lu, P. Li, X. Guo, W. Shi, and J. Liu, Vibration control using ATMD and site measurements on the Shanghai World Financial Center Tower, *The Structural Design of Tall and Special Buildings*, 23, 2014.

[12] I. Nagashima, R. Maseki, Y. Asami, J. Hirai, and H. Abiru, Performance of hybrid mass damper system applied to a 36-storey high-rise building, *Earthquake Engineering and Structural Dynamics*, 30, 11, 2001.

[13] F. Bontempi, F. Casciati, and M. Giudici, Seismic response of a cable-stayed bridge: Active and passive control systems (benchmark problem), *Journal of Structural Control*, 10, 3–4, 2003.

[14] J. N. Yang, S. Lin, and F. Jabbari, H2-based control strategies for civil engineering structures, *Journal of Structural Control*, 10, 2003.

[15] J. N. Yang, A. K. Agrawal, B. Samali, and J.-C. Wu, Benchmark Problem for Response Control of Wind-Excited Tall Buildings, 130, 2004.

[16] C. Meinhardt, N. Nikitas, and D. Demetriou, Application of a 245 metric ton Dual-Use Active TMD System, *Procedia Engineering*, 199, 2017.
[17] J. P. Den Hartog, *Mechanical Vibrations*, 4th ed. New York, NY, USA: McGraw-Hill, 1956.
[18] ANCO ENGINEERS, Users Guide: GERB TMD Tower Control System, 2017.
[19] W. L. Qu, Z. H. Chen, and Y. L. Xu, Dynamic analysis of wind-excited truss tower with friction dampers, *Computers and Structures*, 79, 32, 2001.
[20] T. Soong, Active Structural Control: Theory and Practice, ISBN: 9780582017825, 1990.
[21] S. C. Patwardhan, A Gentle Introduction to Model Predictive Control (MPC) Formulations based on Discrete Linear State Space Models, 2014.
[22] Wikimedia Commons contributors, File:MPC scheme basic.svg, *Wikimedia Commons, the free media repository*, 2018. [accessed 15 June 2020].
[23] J. Löfberg, YALMIP: A toolbox for modeling and optimization in MATLAB, *Proceedings of the IEEE International Symposium on Computer-Aided Control System Design*, 2004.
[24] Gurobi Optimization, LLC, Gurobi Optimizer Reference Manual, http://www.gurobi.com, 2020. [accessed 15 June 2020].